

Quantum phase transition in the Yukawa-SYK model

Yuxuan Wang^{1,*} and Andrey V. Chubukov^{2,†}

¹*Department of Physics, University of Florida, Gainesville, Florida 32601, USA*

²*School of Physics and Astronomy and William I. Fine Theoretical Physics Institute, University of Minnesota, Minneapolis, Minnesota 55455, USA*



(Received 15 May 2020; revised 30 June 2020; accepted 1 July 2020; published 16 July 2020)

We study the quantum phase transition upon varying the fermionic density ν in a solvable model with random Yukawa interactions between N bosons and M fermions, dubbed the Yukawa-SYK model. We show that there are two distinct phases in the model: an incompressible state with gapped excitations and an exotic quantum-critical, non-Fermi liquid state with exponents varying with ν . We show analytically and numerically that the quantum phase transition between these two states is first-order, as for some range of ν the NFL state has a negative compressibility. In the limit $N/M \rightarrow \infty$, the first-order transition gets weaker and asymptotically becomes second-order, with an exotic quantum-critical behavior. We show that fermions and bosons display highly unconventional spectral behavior in the transition region.

DOI: [10.1103/PhysRevResearch.2.033084](https://doi.org/10.1103/PhysRevResearch.2.033084)

I. INTRODUCTION

The non-Fermi liquid (NFL) is one of the most fascinating phenomena in modern condensed matter physics. It violates the fundamental Landau paradigm that quasiparticles must become weakly damped at low enough energies. The key feature of a NFL is a power-law form of the fermionic self-energy, $\Sigma(\omega) \propto \omega^x$ with $x < 1$, which leads to the vanishing of the quasiparticle residue at $\omega = 0$. The NFL behavior has been observed in quite a few unconventional superconducting materials [1–5]. It is widely believed to develop for itinerant fermions near density-wave or $q = 0$ instabilities in either spin or charge channels [6–17], and in systems with fermionic excitations coupled to emergent gauge fields [18–22], such as in quantum spin liquids and half-filled Landau levels.

The theoretical understanding of a NFL remains a challenge. Most of earlier studies of NFLs considered itinerant fermions coupled to soft bosonic modes near a quantum-critical point (QCP). These models show nontrivial NFL behavior at the one-loop order, however in most cases the loop expansion is not controlled because of logarithmic singularities, even in the large N limit, [12, 15], and one has to introduce additional modifications to the model [23–25], e.g., dimension regularization or matrix large- N , to keep the calculations under control. Another route to NFL, which has emerged recently [26–30], explores Sachdev-Ye-Kitaev (SYK)-type models [31–37]. These models describe randomly interacting fermions in a quantum dot. The advantage of SYK model is that it is exactly solvable in the large- N limit and displays

NFL behavior with a particular fractional exponent $x = 1/2$ for the self-energy. Besides, the SYK model has a hidden holographic connection to quantum black holes [32, 33, 33, 38] and in this respect is a simple prototypical model for both NFL and quantum gravity.

In this communication, we consider the generalization of the SYK model, the Yukawa-SYK (Y-SYK) model [39–41], in which M flavors of dispersion-less fermions in a quantum dot randomly interact with N flavors of massive bosons, e.g., optical phonons or gapped collective spin or charge fluctuations. The interest to this model has been triggered by its rich and unconventional physics, and by recent experimental discoveries of strongly correlated behavior in flat band systems like magic angle twisted bilayer graphene [42, 43] and d_{xy} band in Fe-based superconductors [44]. The Y-SYK model has been earlier studied at half-filling [39, 40, 45]. It was shown that the interaction “self-tunes” the system into a NFL, quantum-critical (QC) regime, despite that a bare bosonic mass is finite. This QC regime may in turn become unstable towards non-BCS superconductivity [39–41, 46–49, 28, 50, 51]. Like the SYK model, the Y-SYK model also saturates the upper bound for the onset rate of quantum chaos [52], indicating the existence a classical holographic dual.

We report the results of on the Y-SYK model away from half-filling, at fermionic density $\nu \neq 1/2$. For small deviations from $\nu = 1/2$, we analytically obtain low-energy forms of the fermionic and bosonic Green’s functions with NFL exponents and show that the fermionic self-energy and the spectral function become asymmetric in frequency. At $\nu = 1$, we show that fermions form an incompressible state and bosons remain gapped. We then focus on the quantum phase transition between the compressible NFL state and the incompressible state. We show both analytically and numerically that the phase transition is generally first-order because the chemical potential is a nonmonotonic function of ν , and the compressibility $d\nu/d\mu < 0$ for a range of ν . We argue that this is due to robust low-energy properties of the Y-SYK model. In the transition region, the fermionic and bosonic spectral functions

*yuxuan.wang@ufl.edu

†achubuko@umn.edu

Published by the American Physical Society under the terms of the [Creative Commons Attribution 4.0 International](https://creativecommons.org/licenses/by/4.0/) license. Further distribution of this work must maintain attribution to the author(s) and the published article’s title, journal citation, and DOI.

displays a peculiar precursor behavior [53]. In the particular limit, where the number of bosonic flavors well exceeds the number of fermionic ones, nonmonotonicity disappears and the transition becomes second-order. Even in this case, bosons displays a highly nontrivial “gap filling” behavior: the bosonic mass gap remains finite on both sides of the transition, but on the NFL side of the transition the spectral weight develops around zero energy, and the width of the range, where this happens, increases as the system moves deeper into the NFL region. Taken together, these results reveal rich and universal behavior of zero-dimensional quantum-critical NFL systems.

Some features of the Y-SYK model, like the asymmetry of fermionic self-energy $\Sigma(i\omega)$, are similar to those of the complex SYK model [37,54]. Recent numerical results [55,56] for this model suggest that it may also undergo a first-order quantum phase transition between a NFL state and an insulating state. However, the analytical understanding of that transition is still lacking. In particular it remains unclear whether the first-order transition is a universal property of the complex SYK model, or it depends on nonuniversal aspects of the system behavior at larger frequencies.

II. THE MODEL

The Y-SYK model describes M flavors of dispersion-less fermions, randomly coupled to N flavors of bosons, each with a finite mass m_0 . The dynamics of the model on the Matsubara axis is described by the Lagrangian

$$L = \sum_{i,j=1}^M [c_i^\dagger (\partial_\tau - \mu) c_i] + \sum_{\alpha=1}^N \left[\frac{1}{2} (\partial_\tau \phi_\alpha)^2 + \frac{m_0^2}{2} \phi_\alpha^2 \right] + \frac{i}{\sqrt{MN}} \sum_{ij\alpha} t_{ij}^\alpha c_i^\dagger c_j \phi_\alpha \quad (t_{ij}^\alpha = -t_{ji}^\alpha), \quad (1)$$

where $\{i, j\}$ are fermion flavor indices, $\{\alpha\}$ labels the bosons, and μ is the chemical potential. We have kept the spin indices implicit. In an open system μ is a free (input) parameter, while in a closed system its value is set by the fermionic density per flavor $\nu \equiv \langle c_i^\dagger c_i \rangle$. The Yukawa fermion-boson coupling is assumed to be random: $\langle t_{ij}^\alpha \rangle = 0$, $\langle t_{ij}^\alpha t_{kl}^\beta \rangle = (\delta_{ik} \delta_{jl} + \delta_{il} \delta_{jk}) \delta^{\alpha\beta} \omega_0^3$. We assume ω_0 to be positive. We have chosen the Yukawa coupling to be imaginary, such that the effective interaction in the Cooper channel is repulsive [39,40]. The model has an exact particle-hole symmetry, under which $\mu \rightarrow -\mu$. For definiteness, we set $\mu > 0$. Previous studies have focused on the system at the half filling $\nu = 1/2$, in which case $\mu = 0$.

The model has three energy scales: the bare mass of a boson m_0 , the strength of the Yukawa coupling ω_0 , and the chemical potential μ . We will focus on the “weak-coupling limit” $\omega_0 \ll m_0$. We will see that in this limit there are only two relevant energies, μ and $\omega_F = \omega_0^3/m_0^2$. We emphasize that already at weak coupling, the system behavior at low energies is highly nonperturbative and includes self-tuned criticality and NFL. We work at $T = 0$ and take both M and N as large numbers, but keep the ratio N/M is a parameter.

At the bare level, bosons are gapped, and fermions are free dispersionless quasiparticles. Our goal is to find the fully dressed bosonic and fermionic propagators $G^{-1}(i\omega) = i\omega + \Sigma(i\omega) + \mu$ and $D^{-1}(i\Omega) = \Omega^2 + \Pi(i\Omega) + m_0^2$. We extended

results of earlier analysis at half-filling [39–41] to $\mu \neq 0$ and found that for $M, N \gg 1$ the fermionic and bosonic self-energies are expressed self-consistently via the Schwinger-Dyson equations

$$\begin{aligned} \Pi(i\Omega) &= \frac{2M}{N} \omega_0^3 \int_\omega G(i\omega - i\Omega/2) G(i\omega + i\Omega/2), \\ \Sigma(i\omega) &= -\omega_0^3 \int_\omega D(i\Omega) G(i\omega - i\Omega). \end{aligned} \quad (2)$$

where $\int_\omega \equiv \int d\omega/(2\pi)$.

We first show that the system behavior is qualitatively different at larger μ and at smaller μ , and then consider the phase transition between the two phases by tuning $\mu(\nu)$ in an open (closed) system.

III. INCOMPRESSIBLE GAPPED PHASE AT LARGE μ

The point of departure for the analysis at large μ is the observation that within a direct perturbative expansion the bosonic polarization

$$\Pi(i\Omega) \sim \int_\omega \frac{1}{i(\omega + \Omega/2) + \mu} \frac{1}{i(\omega + \Omega/2) + \mu} = 0 \quad (3)$$

because the poles of the integrand are in the same frequency half-plane. Using bare $D(i\Omega) = 1/(\Omega^2 + m_0^2)$, we obtain for the fermionic self-energy

$$\Sigma(i\omega) = -\int_\Omega \frac{\omega_0^3}{\Omega^2 + m_0^2} \frac{1}{i(\omega - \Omega) + \mu} \approx -\omega_F/2. \quad (4)$$

Substituting this into (2), we find $G(i\omega) = 1/(i\omega + (\mu - \mu^*))$, where $\mu^* = \omega_F/2$. The self-energy comes from low-energy fermions and remains the same if we compute it self-consistently. Similarly, $\Pi(i\Omega)$ still vanishes if we re-evaluate it with dressed fermionic Green’s functions [57]. This self-consistent approach is valid as long as fermions are gapped, i.e., $\mu > \mu^*$. At smaller μ , such solution does not exist, as one can easily verify. Because fermionic energies are all negative, the filling $\nu = 1$ independent on $\mu > \mu^*$, hence this phase is incompressible (the compressibility $dv/d\mu = 0$).

IV. NFL PHASE AT SMALLER μ

At half-filling ($\nu = 1/2$, $\mu = 0$), previous studies have found that $\Pi(i\Omega) + m_0^2 \propto |\Omega|^{1-2x_0}$ and $\Sigma(i\omega) + \mu \propto i|\omega|^{x_0} \text{sgn } \omega$, where x_0 is a function of N/M , ranging from $x_0 = 1/2 - (M/2\pi N)^{1/2}$ at $N/M \rightarrow \infty$ to $x_0 = 0$ at $N/M \rightarrow 0$ ($x_0 = 0.16$ for $N = M$, see Eq. (6) below). This NFL behavior holds at small frequencies for *any* m_0 and *any* nonzero ω_F . Note that $\Pi(0) = -m_0^2$, i.e., the dressed bosonic mass vanishes. This implies that the system self-tunes to quantum critical regime, despite that the bare mass is large compared to the strength of the interaction ($m_0 \gg \omega_0$).

For a nonzero μ , we find that bosons remain massless and fermions retain NFL behavior, but fermionic self-energy becomes an asymmetric function of ω . Specifically, for $\Omega, \omega \ll \omega_F$,

$$\begin{aligned} \Sigma(i\omega) + \mu &\equiv \tilde{\Sigma}(i\omega) = \omega_f \left| \frac{\omega}{\omega_f} \right|^x (i \text{sgn}(\omega) + \alpha), \\ \Pi(i\Omega) + m_0^2 &\equiv \tilde{\Pi}(i\Omega) = \beta m_0^2 \left| \frac{\Omega}{\omega_f} \right|^{1-2x}, \end{aligned} \quad (5)$$

where α parametrizes spectral asymmetry [54] and ω_f is the NFL energy scale, below which $|\Sigma(i\omega)| < \omega$. Altogether we have four dimensionless parameters: x , α , β , and ω_f/ω_F . Substituting these forms into Eq. (2) and matching the power-law parts $\tilde{\Sigma}$ and $\tilde{\Pi}$, we obtain two equations: (see Appendix A)

$$(1 - \alpha^2) \frac{1 + \sec \pi x}{1/x - 2} + \frac{2\alpha^2}{1/x - 2} = (1 + \alpha^2) \frac{N}{2M}, \quad (6)$$

$$\frac{\omega_F}{4\pi\beta\omega_f(1 + \alpha^2)} \frac{\Gamma^2(-x)}{\Gamma(-2x)} = -1. \quad (7)$$

These relations are exact as relevant fermionic and bosonic frequencies in (2) are comparable to external ω and Ω , which we set to be much smaller than ω_f . Note that the matching the real and the imaginary parts of $\tilde{\Sigma}(i\omega)$ gives the same equation. Physical values of the exponent x in (6) and (7) are $x \leq 1/2$. A larger x would lead to negative $\beta\omega_f$, which violates the unitarity of the theory. For $x \rightarrow 1/2$, $\alpha \rightarrow 1$ ($\alpha - 1 \approx \pi(1/2 - x)$). At half-filling, $\alpha = 0$ and $x = x_0$ is a function of M/N ($x_0 \approx 0.16$ at $M/N = 1$). The two other conditions are $\Sigma(0) = -\mu$ and $\Pi(0) = -m_0^2$. Using Eq. (2), we obtain

$$\frac{\mu}{\omega_F} = \int_{\omega} \frac{1}{i\omega + \tilde{\Sigma}(\omega)} \frac{1}{\omega^2 + \tilde{\Pi}(\omega)}, \frac{1}{\omega_F} = \int_{\omega} \frac{-2M/N}{(i\omega + \tilde{\Sigma}(\omega))^2}. \quad (8)$$

Substituting $\Sigma(i\omega)$ and $\Pi(i\Omega)$ from (5), we obtain

$$\beta = F_1(x), \quad \alpha = \frac{\mu}{\omega_F} F_2(x). \quad (9)$$

The functions $F_{1,2}(x)$ are regular $\mathcal{O}(1)$ functions of the argument, and $F_1(1/2) = 1$, $F_2(1/2) = 1/2$. We present them in Appendix A1. The relations (9) are not exact, because relevant ω in (8) are of order ω_f . For these ω , Eqs. (5) are valid up to corrections $\mathcal{O}(1)$, as the forms of $\Sigma(i\omega)$ and $\Pi(i\Omega)$ change at $\omega, \Omega > \omega_f$: the bosonic self-energy gradually decreases and the fermionic $\Sigma(\omega)$ acquires a Fermi liquid form [58]. Nevertheless, we find that the relations $F_1(1/2) = 1$ and $F_2(1/2) = 1/2$ are actually exact (see Appendix A1), i.e., at $x = 1/2$, $\mu = \mu^* = \omega_F/2$.

While α cannot be universally expressed via the chemical potential, it can be exactly expressed via the density ν . Using the Luttinger relation between ν and properly regularized $\int G(i\omega)d\omega$, we obtain (see Appendix B)

$$\nu = \frac{1}{2} + \frac{\tan^{-1} \alpha}{\pi} + \frac{x}{2 \sin(\pi x)} \frac{2\alpha}{1 + \alpha^2}. \quad (10)$$

The same relation holds for the complex SYK model [37,54]. From Eqs. (10) and (7), we see that as $x \rightarrow 1/2$ and $\alpha \rightarrow 1$, the filling ν approaches 1 and ω_f tends to zero. This implies that the range of NFL behavior vanishes at $\nu \rightarrow 1$.

Combining Eqs. (6), (9), and (10), we obtain α and μ as functions of the filling ν . We plot these two functions for $M = N$ in Fig. 1. We see that both α and μ are nonmonotonic functions of ν , and there is a range of ν where the compressibility $dv/d\mu$ is negative. The relation $\alpha(\nu)$ is exact, the other one, $\mu(\nu)$, is approximate, as to get it we used Eq. (9). To verify that the nonmonotonic behavior of μ is not the artifact of our approximation, we iteratively solved the nonlinear integral equations (2) for $\Sigma(i\omega)$ and $\Pi(i\Omega)$ for all

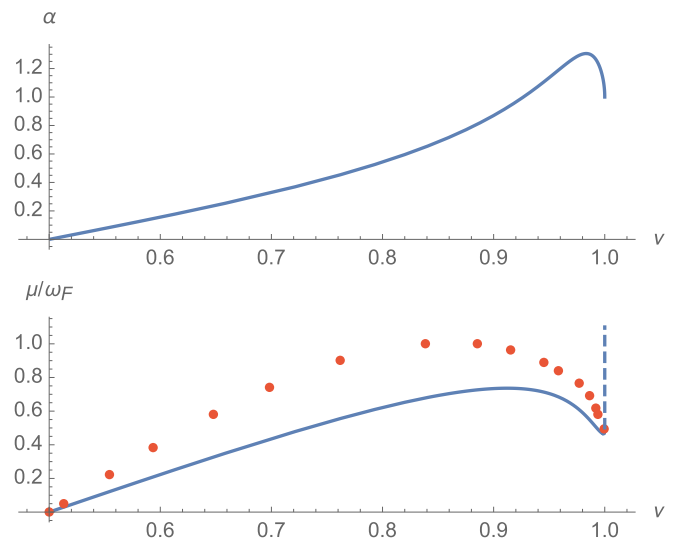


FIG. 1. (Top) The dependence of the spectral asymmetry parameter α on the filling ν . (Bottom) The qualitative (solid line) and numerical (red dots) dependence of the chemical potential μ on the filling ν . The solid line was obtained by using the low-energy form (5) for the self-energies for all frequencies. The vertical dashed line in the lower panel represents the incompressible phase. We set $N = M$, in which case $x_0 = 0.16$. The solid line actually has a minute dip at $\nu \approx 0.98$ (see Appendices A1 and B). It is not present in the full numerical solution and likely is an artifact of using Eq. (5) at all energies.

frequencies, using the analytical power-law forms in (5) as an input. We show the numerical results [59] for $\mu(\nu)$ for $M = N$ in Fig. 1. We see that the nonmonotonic behavior persists.

V. QUANTUM PHASE TRANSITION

The existence of a range of densities, where $\partial\nu/\partial\mu$ is negative, implies that the NFL solution is unstable, and the transition between the NFL and the insulating state must be first-order. In an open system, there is a discontinuous transition to the incompressible phase [60] at some critical μ_c . In a closed system, there is a phase coexistence region, in which the system displays simultaneously gap features from the incompressible state and NFL features at small frequencies [see Fig. 2(a)]. This resembles the ‘‘gap filling’’ behavior near a Mott transition at $T = 0$ [53].

At $N \gg M$ the range, where $\mu(\nu)$ is nonmonotonic, shrinks [this follows from Eq. (6)], and the transition becomes weakly first-order. We show this behavior in Fig. 3 for $N/M = 60$. We expect that at $N/M \rightarrow \infty$ the transition becomes second order at $\nu = 1$ (and $\mu = \omega_F/2$, $x = 1/2$, $\alpha = 1$). In this case, there exists a quantum-critical point that separates a gapless NFL phase (which is by itself quantum critical) and an incompressible, insulating phase. This transition has an unconventional feature on its own: the peak in the bosonic $D(\Omega)$ at $\Omega = m_0$ is present on both sides of the transition. In addition, a nonzero bosonic spectral weight builds up at small frequencies in the NFL phase and progressively takes the spectral weight from the peak at m_0 . The behavior of the fermionic spectral function is more conventional: the gap in the fermionic spectral function $\mu - \omega_F/2$ vanishes at the

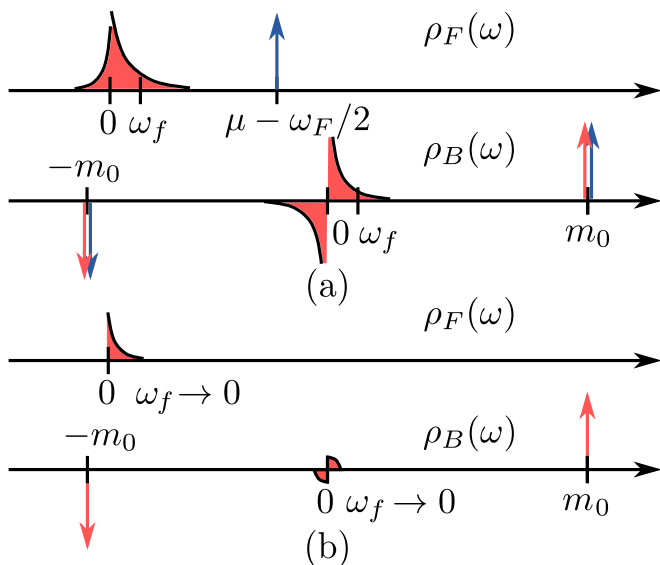


FIG. 2. Schematic bosonic and fermionic spectral functions, $\rho_F(\omega) \equiv -\text{Im} G(\omega + i\eta)$ and $\rho_B(\omega) \equiv \text{Im} D(\omega + i\eta)$, at the first-order transition for $N \sim M$ (a), and at the second-order transition for $N/M \rightarrow \infty$ (b). The vertical arrows represent δ -function peaks. The blue and red peaks in (a) come from the coexisting phases: the NFL phase (red) and the incompressible phase (blue).

transition and an asymmetric spectral weight builds in the NFL phase. We show the behavior of the spectral functions in Fig. 2(b) and present more details in Appendix C.

VI. SUMMARY

In this communication, we analyzed the behavior of M flavors of fermions, randomly interacting with N flavors of massive bosons (the Y-SYK model) away from half-filling. We showed that the system can be in one of the two phases—a NFL phase with asymmetrically broadened spectral weight, and an incompressible gapped phase. We studied the quantum

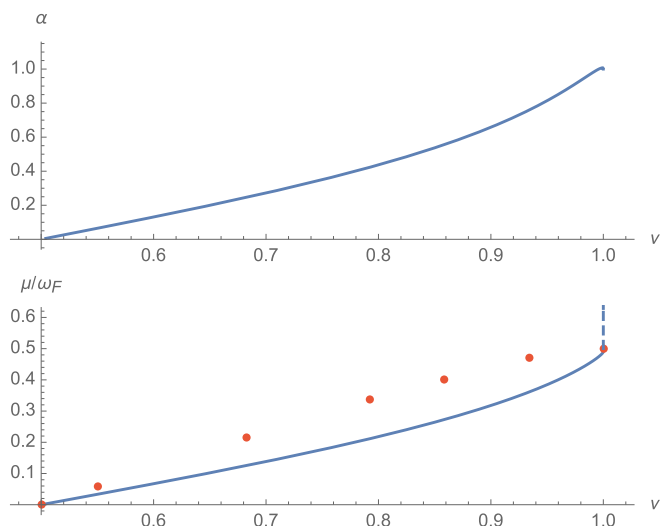


FIG. 3. Same as in Fig. 1, but for $N = 60M$. In this case, $x_0 = 0.45$.

phase transition between these two phases upon the variation of fermionic density. We showed by analytical and numerical calculations that the transition is in general first-order, but becomes second-order in the limit $N/M \rightarrow \infty$. In the case of the first-order transition, there is a gap filling behavior in the transition region in both fermionic and bosonic sectors. For the second order transition, fermionic gap closes at the transition, but the bosonic spectral function still displays a gap filling behavior.

Recent numerical studies [55,56] of the complex SYK model also indicated that the system undergoes a first-order transition upon varying the density. In distinction to our analysis, there the NFL exponent x is fixed, while in our case it varies with the filling. The possibility of a second-order transition at $N/M \rightarrow \infty$ was not addressed in these numerical studies.

We conclude by listing several open questions. First, in our analysis we focused on the case $T = 0$. It is possible that at a finite T the first-order transition extends to a line, which terminates at a classical critical point, like in a water-vapor phase diagram. Second, we analyzed the two-point Green’s functions. It will be interesting to examine the behavior of four-point functions, possibly using the conformal reparametrization symmetry of the low-energy theory. This will shed light on the issue of the strength of superconducting and charge fluctuations. Third, we focused on the weak-coupling case, $\omega_0 \ll m_0$. At strong coupling, the analysis becomes more involved, even though the large M, N limit still guarantees the validity of the self-consistent Schwinger-Dyson equations. It has been pointed out that purely bosonic SYK-like models may exhibit glassy behavior at low temperatures [61,62]. It would be interesting to see if that happens at strong coupling in Y-SYK model. Finally, in terms of measurable quantities, e.g., in transport experiments, we note that recently it has been proposed that the thermoelectric power [63], measured in quantum matter systems, can be a direct probe of the Bekenstein-Hawking entropy of the SYK models. In SYK-like models it has also been argued that the soft reparametrization modes lead to a universal linear-in-temperature resistivity [64]. We also note that these transport quantities can be studied using determinant quantum Monte Carlo methods, since the Y-SYK model is free from the fermion sign problem [45]. We leave the analysis of the transport properties in the Y-SYK model to future work.

ACKNOWLEDGMENTS

We thank L. Classen, I. Esterlis, Z. Meng, A. Kamenev, S. Kivelson, S. Sachdev, J. Schmalian, P. Zhang, and especially Y. Gu for illuminating discussions. This research was initiated at Stanford University through the Gordon and Betty Moore Foundation’s EPiQS Initiative through Grants GBMF4302 and GBMF8686, and at the Aspen Center for Physics, supported by NSF PHY-1066293. A.V.C. is supported by the NSF DMR-1834856. Y.W. is supported by startup funds at University of Florida.

Appendix is organized as follows. In Sec. A, we provide details on the power-law solution of the bosonic and fermionic self-energies at low frequencies. In Sec. A 1, we discuss the analytical solution of the chemical potential μ by extending

the low-energy power-law expression for the self-energies to all frequencies. Despite not being self-consistent at high-energies, we argue that it captures the correct qualitative behavior. In Sec. A 2, we analyze the behavior of the self-energies at high frequencies. In Sec. B, we derive an exact relation between the fermionic filling number ν and the low energy behavior of the fermionic Green's function. In Sec. C, we analyze the behavior of the bosonic and fermionic spectral functions at the endpoint of the NFL state and prove that the relation obtained in Sec. A 1 is exact.

APPENDIX A: DETAILS ON THE NFL SOLUTION

For the self-energies at low frequencies, we take the ansatz

$$\begin{aligned}\tilde{\Sigma}(i\omega) &\equiv \Sigma(i\omega) - \Sigma(0) = \omega_f \left| \frac{\omega}{\omega_f} \right|^x (i \operatorname{sgn}(\omega) + \alpha), \\ \tilde{\Pi}(i\Omega) &\equiv \Pi(i\Omega) - \Pi(0) = \beta m_0^2 \left| \frac{\Omega}{\omega_f} \right|^{1-2x}.\end{aligned}\quad (\text{A1})$$

$$\beta m_0^2 \left| \frac{\Omega}{\omega_f} \right|^{1-2x} = \frac{2M\omega_0^3}{N\omega_f^2} \int \left[\frac{(-i \operatorname{sgn}(\omega) + \alpha)(-i \operatorname{sgn}(\omega + \Omega) + \alpha)\omega_f^{2x}}{(1 + \alpha^2)^2 |\omega|^x |\omega + \Omega|^x} - \frac{(\alpha^2 - 1)\omega_f^{2x}}{(1 + \alpha^2)^2 |\omega|^{2x}} \right] \frac{d\omega}{2\pi}, \quad (\text{A6})$$

from which we obtain

$$1 = -\frac{M\omega_F}{N\pi\beta\omega_f(1 + \alpha^2)^2} \left[(1 - \alpha^2) \frac{\Gamma^2(-x)}{2\Gamma(-2x)} \frac{(1 + \sec \pi x)}{1/x - 2} + 2\alpha^2 \frac{\Gamma^2(-x)}{2\Gamma(-2x)} \frac{1}{1/x - 2} \right]. \quad (\text{A7})$$

From Eq. (A5), we have

$$\omega_f [i \operatorname{sgn}(\omega) + \alpha] |\omega|^x = -\frac{\omega_0^3}{2\pi\beta m_0^2} \int \left[\frac{\alpha - i \operatorname{sgn}(\Omega)}{\alpha^2 + 1} |\Omega|^{-x} |\omega - \Omega|^{2x-1} - \frac{\alpha}{\alpha^2 + 1} |\Omega|^{x-1} \right] d\Omega. \quad (\text{A8})$$

The real and imaginary parts actually yield a single equation: indeed, for real and imaginary parts, we get respectively

$$\begin{aligned}1 &= -\frac{\omega_F}{2\pi\beta\omega_f(1 + \alpha^2)} \int \left(\frac{1}{|y|^x |1 - y|^{1-2x}} - \frac{1}{|y|^{1-x}} \right) dy, \\ 1 &= \frac{\omega_F}{2\pi\beta\omega_f(1 + \alpha^2)} \int \frac{\operatorname{sgn}(y) dy}{|y|^x |1 - y|^{1-2x}}.\end{aligned}\quad (\text{A9})$$

It is straightforward to verify that they lead to a single constraint:

$$1 = -\frac{\omega_F}{4\pi\beta\omega_f(1 + \alpha^2)} \frac{\Gamma^2(-x)}{\Gamma(-2x)}. \quad (\text{A10})$$

Combining (A7) and (7), we get

$$(1 - \alpha^2) \frac{(1 + \sec \pi x)}{1/x - 2} + \frac{2\alpha^2}{1/x - 2} = \frac{N}{2M} (1 + \alpha^2), \quad (\text{A11})$$

Equations (A10) and (A11) are Eqs. (6) and (7) in the main text.

In evaluating the integrals above, we have made use of

$$\int \frac{\operatorname{sgn}(y) dy}{|y|^x |1 - y|^{1-2x}} = -\frac{\Gamma^2(-x)}{2\Gamma(-2x)}, \quad (\text{A12})$$

There are four dimensionless parameters to solve for α , β , x , and ω_f/ω_F . There are also four equations:

$$\Sigma(0) = -\mu = -\frac{\omega_0^3}{2\pi} \int \frac{d\omega}{i\omega + \tilde{\Sigma}(\omega)} \frac{1}{\tilde{\Pi}(\omega)}, \quad (\text{A2})$$

$$\Pi(0) = -m_0^2 = \frac{2M}{N} \frac{\omega_0^3}{2\pi} \int \frac{d\omega}{(i\omega + \tilde{\Sigma}(\omega))^2}, \quad (\text{A3})$$

$$\begin{aligned}\beta m_0^2 \left| \frac{\Omega}{\omega_f} \right|^{1-2x} &= \frac{M\omega_0^3}{N\pi} \int [\tilde{\Sigma}^{-1}(i\omega) \tilde{\Sigma}^{-1}(i\omega + i\Omega) \\ &\quad - \tilde{\Sigma}^{-2}(i\omega)] d\omega,\end{aligned}\quad (\text{A4})$$

$$\begin{aligned}(i \operatorname{sgn}(\omega) + \alpha) \omega_f \left| \frac{\omega}{\omega_f} \right|^x &= -\frac{\omega_0^3}{2\pi} \int [\tilde{\Sigma}^{-1}(i\Omega) \tilde{\Pi}^{-1}(i\Omega - i\omega) \\ &\quad - \tilde{\Sigma}^{-1}(i\Omega) \tilde{\Pi}^{-1}(i\Omega)] d\Omega.\end{aligned}\quad (\text{A5})$$

In this section, we self-consistently solve Eqs. (A4) and (A5). Since the integrals are fully convergent using (A1), the relations we obtain are independent of the high-energy nonuniversal details. From Eq. (A4), we have

$$\begin{aligned}\int dy \left[\frac{\operatorname{sgn}(y + 1/2) \operatorname{sgn}(y - 1/2)}{|y + 1/2|^x |y - 1/2|^x} - \frac{1}{|y|^{2x}} \right] \\ = \frac{\Gamma^2(-x)}{2\Gamma(-2x)} \frac{(1 + \sec \pi x)}{1/x - 2},\end{aligned}\quad (\text{A13})$$

$$\int_{-1/2}^{1/2} \frac{dy}{|y + 1/2|^x |y - 1/2|^x} = -\frac{\Gamma^2(-x)}{2\Gamma(-2x)} \frac{1}{1/x - 2}. \quad (\text{A14})$$

1. The other two equations on the parameters

We now consider the other two equations, Eqs. (1) and (4). One can easily verify that relevant frequencies in the integrals over ω in the right-hand side of these two equations are of order ω_f . At such frequencies, the corrections to the power-law forms in Eq. (A1) are of order one. To find the exact values of the integrals in (1) and (4) one then needs to know the full forms of $\Sigma(i\omega)$ and $\Phi(i\omega)$. We found the full forms numerically and combined the numerical results with the two exact relations, Eqs. (7) and (6) to obtain the expressions for x , α , β , and ω_f/ω_F as functions of μ . We then used the additional exact relation between the filling μ and α and expressed μ as a function of ν (the dotted lines in Figs. 1 and 2 in the main text).

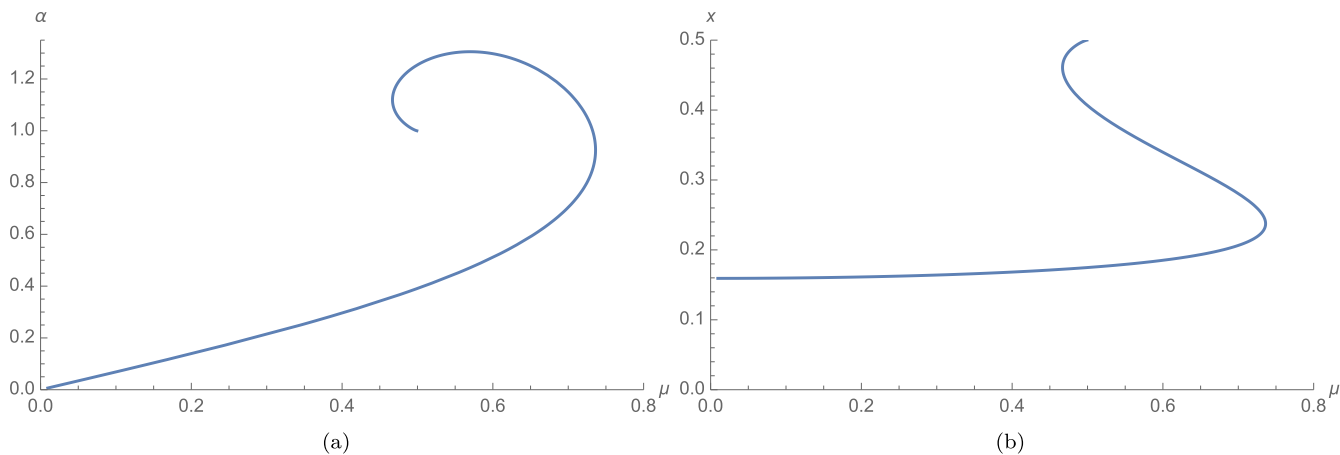


FIG. 4. The functions $\alpha(\mu)$ and $x(\mu)$ for $M = N$ obtained in Sec. A 1.

Here, we obtain the approximate analytical relations from Eqs. (1) and (4) by keeping the power-law forms of the bosonic and fermionic self-energies. The integrals on the right hand side of (1) and (4) are ultraviolet convergent because of the bare ω in the fermionic propagator. Evaluating the integrals, we obtain

$$\beta = \frac{1}{4^{x-1}} \frac{\Psi_3(x, \alpha)}{\Psi_1(x, \alpha)}, \quad \alpha = \frac{\mu}{\omega_F} \frac{4^x}{8} \frac{\Psi_3(x, \alpha)}{\Psi_1(x, \alpha)\Psi_2(x, \alpha)}, \quad (\text{A15})$$

where

$$\begin{aligned} \Psi_1(x, \alpha) &= \frac{M}{N\pi} \int_0^\infty \frac{dy}{y^{2x}} \frac{(1 + y^{1-x})^2 - \alpha^2}{((1 + y^{1-x})^2 + \alpha^2)^2}, \\ \Psi_2(x, \alpha) &= \frac{1}{2\pi} \int_0^\infty \frac{dy}{y^{1-x}} \frac{1}{(1 + z^{1-x})^2 + \alpha^2}, \\ \Psi_3(x, \alpha) &= -\frac{M}{2N\pi} \frac{1}{4^x(1 + \alpha^2)} \frac{\Gamma^2(-x)}{\Gamma(-2x)}. \end{aligned} \quad (\text{A16})$$

In the last line in (A16), we used the exact relation (6). This relation also allows one to express the spectral asymmetry parameter α via the exponent x (or vice versa), hence $\Psi_{1,2,3}$ are in fact the functions of only one variable. As a consequence, we can write

$$\beta = F_1(x), \quad \alpha = \frac{\mu}{\omega_F} F_2(x), \quad (\text{A17})$$

where $F_1(x) = 4^{x-1}\Psi_3(x, \alpha(x))/\Psi_1(x, \alpha(x))$ and $F_2(x) = 2^{2x-3}\Psi_3(x, \alpha(x))/(\Psi_1(x, \alpha(x))\Psi_2(x, \alpha(x)))$.

We will see in Sec. B that x gradually increases with increasing filling ν and reaches $x = 1/2$ at maximum possible $\nu = 1$. Equation (6) shows that for $x \rightarrow 1/2$, $\alpha \rightarrow 1$, and $\alpha - 1 \approx \pi(1/2 - x)$. Substituting this into Eq. (A16), we obtain that $\Psi_1(x, \alpha)$ and $\Psi_3(x, \alpha)$ vanish in this limit, but the ratio $\Psi_1(x, \alpha)/\Psi_3(x, \alpha)$ tends to $1/2$. The vanishing of Ψ_1 implies that $\omega_f(x) = 2\omega_F\Psi_1(x, \alpha(x))$ vanishes, i.e., for $x \rightarrow 1/2$, the width of the NFL region shrinks to zero. Simultaneously, $\Psi_2(1/2, 1) = 1/4$, hence $\mu = \omega_F/2$, the same as the boundary of the incompressible phase. Using Eqs. (9), (A16), and (7) and the properties of $\Psi_{1,2,3}$, it is straightforward to verify that the functions $F_{1,2}(x)$ are regular $\mathcal{O}(1)$ functions of x , with

$$F_1(1/2) = 1, \quad F_2(1/2) = 1/2. \quad (\text{A18})$$

Remarkably, both of these special values are exact, as we will show in Sec. C.

In Fig. 4, we plot α and x as functions of μ for $M = N$. We see that both become multivalued functions in some range of μ . This is a clear indication that the transition between the NFL phase and the incompressible phase may be first order, although to fully address this issue we need to know the relation between the filling ν and the chemical potential μ .

2. Behavior of the NFL solution at high energies

In this section, we analyze the behavior of the fermionic and bosonic self-energies in the NFL phase at frequencies larger than the ω_f . For simplicity, here we focus on the case well inside the NFL phase, where ω_f and $\omega_F \equiv \omega_0^3/m_0^2$ are of the same order, which we will use interchangeably for a qualitative analysis.

At $\omega \gg \omega_f$, the fermionic self-energy receives contributions from typical bosonic and fermionic frequencies smaller and greater than ω_f . We assume and verify that above the NFL energy scale, $\omega, \Omega \gg \omega_f$, both the fermionic and bosonic Green's functions take their free forms. We then have

$$\begin{aligned} \Sigma(i\omega) &\sim -\frac{\omega_0^3}{m_0^2} \int_{-\omega_f}^{\omega_f} \frac{d\Omega}{2\pi} \frac{1}{|\Omega/\omega_f|^{1-2x}} \frac{1}{i\omega} - \frac{\omega_0^3}{\omega^2 + m_0^2} \\ &\times \int_{-\omega_f}^{\omega_f} \frac{d\omega'}{2\pi} \frac{1}{(i \operatorname{sgn}(\omega') - \alpha)\omega_f|\omega'/\omega_f|^x} \\ &- \omega_0^3 \int_{\{\Omega_0\}} \frac{d\Omega}{2\pi} \frac{1}{\Omega^2 + m_0^2} \frac{1}{i(\omega - \Omega)}, \end{aligned} \quad (\text{A19})$$

where the integration domain $\{\Omega_0\}$ excludes $\{-\omega_f, \omega_f\} \cap \{\omega - \omega_f, \omega + \omega_f\}$. We have also dropped the chemical potential terms in the bare Green's function, since in the NFL phase $\mu \lesssim \omega_f$ and is subdominant at high frequencies.

The first two integrals are elementary. The third term, in the $\omega_f \ll m_0$ limit can be replaced with a principal value integral

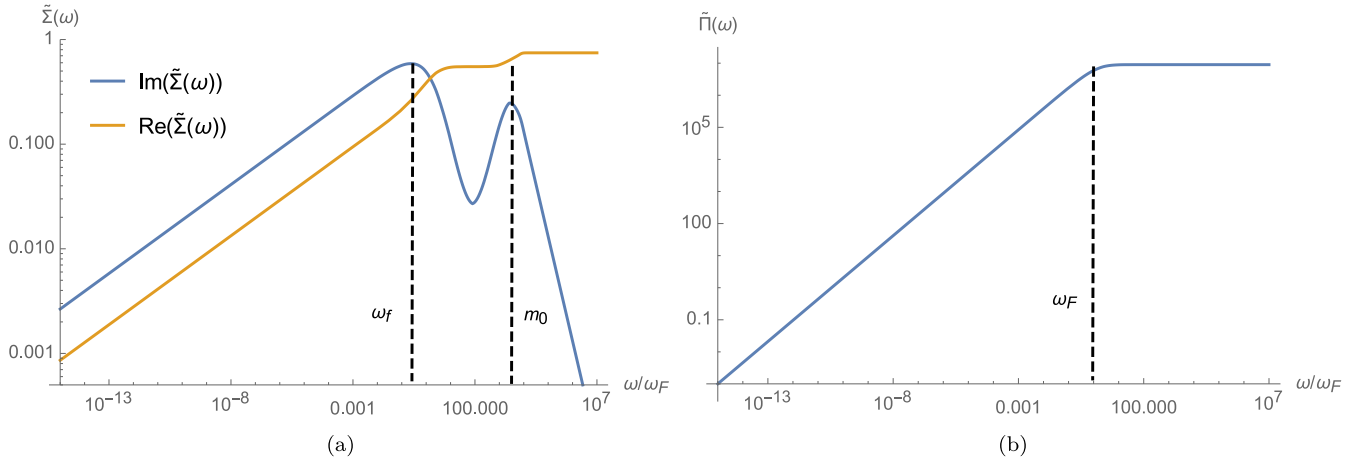


FIG. 5. The full solution $\tilde{\Sigma}(i\omega)$ and $\tilde{\Pi}(i\omega)$ for the Schwinger-Dyson equations. We have taken $m_0 = 3000\omega_f$.

circumventing $\omega = \Omega$. We have

$$\begin{aligned} \Sigma(i\omega) &= ic_1 \frac{\omega_f^2}{\omega} + c_2 \frac{\omega_0^3}{\omega^2 + m_0^2} \frac{\alpha}{1 + \alpha^2} \\ &\quad - \omega_0^3 \int_{-\infty}^{\infty} \frac{d\Omega}{2\pi} \frac{1}{\Omega^2 + m_0^2} \text{P} \left[\frac{1}{i(\omega - \Omega)} \right] \\ &= ic_1 \frac{\omega_f^2}{\omega} + c_2 \frac{\omega_0^3}{\omega^2 + m_0^2} \frac{\alpha}{1 + \alpha^2} + i \frac{\omega_0^3}{m_0} \frac{\omega}{\omega^2 + m_0^2}. \end{aligned} \quad (\text{A20})$$

For $\omega_f \ll \omega \ll \sqrt{\omega_0^3/m_0}$, its asymptotic behavior is given by

$$\Sigma(i\omega) = ic_1 \frac{\omega_f^2}{\omega} + c_2 \frac{\alpha\omega_f}{1 + \alpha^2} = ic_1 \frac{\omega_f^2}{\omega} + \tilde{c}_2\mu, \quad (\text{A21})$$

where in the last step we have used $\mu \sim \alpha\omega_f$. Combined with the result on $\Sigma(i\omega)$ at $\omega \ll \omega_f$, we see that the two asymptotic behaviors do match at $\omega \sim \omega_f$.

For $\omega \gg \sqrt{\omega_0^3/m_0}$, the self-energy has a nonmonotonic behavior, given by

$$\Sigma(i\omega) = c_2 \frac{\omega_0^3}{\omega^2 + m_0^2} \frac{\alpha}{1 + \alpha^2} + i \frac{\omega_0^3}{m_0} \frac{\omega}{\omega^2 + m_0^2}, \quad (\text{A22})$$

in which $\text{Im}(\Sigma(i\omega))$ remains a constant $\sim \mu$ at $\omega \ll m_0$ and decays to zero at $\omega \gg m_0$. On the other hand $\Re(\Sigma(i\omega))$ first increases linearly and then again decreases as $1/\omega$. However, this nonmonotonic behavior in has little effect on the low-energy behaviors of the system. For both regimes above, the self-energy effects in the fermionic Green's function is small, since $\omega \ll |\Sigma(i\omega)|$, thus justifying our assumption that the fermions are essentially free.

For the bosons at $\Omega \gg \omega_f$, the self-energy comes from frequencies $\omega \gg \omega_f$. We have qualitatively

$$\Pi(i\Omega) \sim - \int_{\Omega} \frac{\omega_0^3 d\omega}{\omega^2} \sim \frac{\omega_0^3}{\Omega} \ll m_0^2, \quad \tilde{\Pi}(i\Omega) \approx m_0^2. \quad (\text{A23})$$

We see that the bosons are essentially free in this frequency range.

These results can be directly verified by numerically solving the Schwinger-Dyson equations, using the same iterative

technique sketched in the main text. In Fig. 5, we present the numerical solution for $\tilde{\Sigma}(i\omega)$ and $\tilde{\Pi}(i\omega)$, in which the power-law behavior in different regimes can be easily seen. The $\mathcal{O}(1)$ numerical constants c_1 and c_2 can be fitted from the numerics.

APPENDIX B: LUTTINGER'S THEOREM FOR THE NFL STATE

In this section, we focus on the analytical derivation of the filling fraction ν . From the usual relation

$$\nu = \int_{-i\infty}^{i\infty} \frac{dz}{2\pi i} G(z) e^{z0_+}, \quad (\text{B1})$$

where $G(z) = 1/(z - \tilde{\Sigma}(z))$, it may seem that its value depends on details of the system behavior at high energies, but due to a Luttinger-theorem-like relation it can be shown to be completely determined by low-energy, or infrared (IR), behaviors. This is an example of ultraviolet(UV)-IR mixing, a feature shared in the original complex SYK model, and its mathematical structure is similar to the chiral anomaly in quantum electrodynamics. Our presentation closely parallels that in Ref. [37].

Using the identity $\partial_z(G^{-1}(z) - \tilde{\Sigma}(z)) = 1$, we rewrite ν as

$$\begin{aligned} \nu &= \int_{-i\infty}^{i\infty} \frac{dz}{2\pi i} G(z) e^{z0_+} \\ &= \int_{-i\infty}^{i\infty} \frac{dz}{2\pi i} G(z) e^{z0_+} \partial_z(G^{-1}(z) - \tilde{\Sigma}) \equiv I_1 - I_2. \end{aligned} \quad (\text{B2})$$

The first term I_1 is expressed as

$$\begin{aligned} I_1 &= \int_{-i\infty}^{i\infty} \frac{dz}{2\pi i} G(z) e^{z\delta} \partial_z G^{-1}(z) \\ &= \int_{-i\infty}^{i\infty} \frac{d \ln(G^{-1}(z))}{2\pi i} e^{z\delta}. \end{aligned} \quad (\text{B3})$$

This integral is IR divergent. However, it is clear that in the first equation of (B2) there is no IR divergence, which is convergent at $z = 0$. Thus the IR divergence should cancel when properly regularized. One way to properly regularize

both integrals is to take principle values. For I_1 ,

$$\begin{aligned} I_1 &= -\text{P} \int_{-i\infty}^{i\infty} \frac{d \ln(G^{-1}(z))}{2\pi i} e^{z\delta} \\ &= \left(\int_{-i\eta}^{-\infty-i\eta} - \int_{i\eta}^{-\infty+i\eta} \right) \frac{d \ln(G^{-1}(z))}{2\pi i} \\ &= \frac{\arg(G^{-1}(-i\eta)) - \arg(G^{-1}(-\infty + i\eta))}{\pi} \\ &= \frac{\arg(G^{-1}(-i\eta))}{\pi} - 1 \end{aligned} \tag{B4}$$

where in the second step, we have deformed the integration contour allowed by the $e^{z\delta}$ factor. Interestingly this only depends on IR properties of the Green's functions.

The evaluation of I_2 is more tricky. If we simply use IR expressions for G and $\tilde{\Sigma}$ in

$$I_2 = \int_{-i\infty}^{i\infty} \frac{dz}{2\pi i} G(z) \partial_z \tilde{\Sigma}(z) e^{z\delta}, \tag{B5}$$

the I_2 integral is formally logarithmically divergent. However, the infinities at both the IR and UV ends are canceled by the integration domain (the asymmetry cancels out between G and Σ). All we need is to properly regularize the integral at both ends.

In the standard treatment of Luttinger's theorem [65,66], the I_2 term can be transformed to an integral over a total derivative (of the Luttinger-Ward functional) and thus is zero. In our case however, the integral is not along a continuous path, since we are taking principal values. Across the branch cuts of $G(z)$ there are additional boundary terms, which are divergent. They can be made to exactly cancel each other if we take $e^{z\delta} \rightarrow 1$ prior to the principal value limit, but physically

from the definition of the charge one should take the $e^{z\delta} \rightarrow 1$ limit only *after* the principal value limit. In fact, according to the Riemann rearrangement theorem they can be made to take any value, so the correct order of limits is crucial. From this analysis, we see that the nonzero contribution should come from the IR end, since the boundary terms at infinity is well-behaved and vanishes.

We deform the integration contour in the same way as in I_1 and

$$I_2 = \int_0^{-\infty} \frac{d\omega}{\pi} \text{Im}[G(i\omega) \partial_z \Sigma(i\omega)]|_{i\omega \rightarrow \omega + i\eta} e^{x\delta}. \tag{B6}$$

It is important to not directly replace the integral $\partial_{i\omega}$ with ∂_ω since the self-energy is nonanalytic along the real axis. This integral is well behaved, so we can take the $\delta \rightarrow 0$ limit first. As we will see, the integral converges even if we just use the power-law form for the self-energy, since the UV logarithmical divergence cancels when the integration domain is folded to a half space.

For convenience, let us rewrite our self-energies at small frequencies as

$$\begin{aligned} \tilde{\Sigma}(\pm i\omega) &= \pm i e^{\mp i\theta} \bar{\omega}_f^{1-x} \omega^x, \\ \tilde{\Gamma}(\pm i\Omega) &= \bar{\beta} m_0^2 \left(\frac{\Omega}{\bar{\omega}_f} \right)^{1-2x}, \end{aligned} \tag{B7}$$

where we have defined $\theta = \tan^{-1} \alpha$ and $\bar{\beta} \bar{\omega}_f = (1 + \alpha^2) \beta \omega_f$. The I_1 integral in Eq. (B4) yields

$$I_1 = \frac{1}{2} + \frac{\theta}{\pi}. \tag{B8}$$

It turns out that it is easiest to analyze the I_2 integral using the spectral representation, which gives

$$\begin{aligned} \frac{I_2}{\omega_0^3} &= \int_{-\infty}^0 \frac{d\omega}{\pi} \text{Im} \left[\int \frac{d\omega_1}{\pi} \frac{\rho_F(\omega_1)}{i\omega - \omega_1} \int \frac{d\Omega}{2\pi} \int \frac{d\omega_2 d\omega_3}{\pi^2} \frac{-\rho_F(\omega_2)}{(i\omega - i\Omega - \omega_2)^2} \frac{\rho_B(\omega_3)}{i\Omega - \omega_3} \right] \Big|_{i\omega \rightarrow \omega + i\eta} \\ &= \int_{-\infty}^0 \frac{d\omega}{\pi} \text{Im} \left[\int \frac{d\omega^3}{\pi^3} \frac{\rho_F(\omega_1)}{\omega - \omega_1 + i\eta} \frac{\rho_F(\omega_2) \rho_B(\omega_3)}{(\omega - \omega_2 - \omega_3 + i\eta)^2} (\text{sgn}(\omega_2) + \text{sgn}(\omega_3)) \right] \\ &= - \int_0^{\infty} \frac{d\omega}{\pi} \text{Im} \left[\int \frac{d\omega^3}{\pi^3} \frac{\rho_F(-\omega_1)}{-\omega + \omega_1 - i\eta} \frac{\rho_F(-\omega_2) \rho_B(-\omega_3)}{(-\omega + \omega_2 + \omega_3 - i\eta)^2} (-\text{sgn}(\omega_2) - \text{sgn}(\omega_3)) \right] \\ &= - \int_0^{\infty} \frac{d\omega}{\pi} \text{Im} \left[\int \frac{d\omega^3}{\pi^3} \frac{\rho_F(-\omega_1)}{\omega - \omega_1 + i\eta} \frac{\rho_F(-\omega_2) \rho_B(-\omega_3)}{(\omega - \omega_2 - \omega_3 + i\eta)^2} (\text{sgn}(\omega_2) + \text{sgn}(\omega_3)) \right] \\ &= \int_0^{\infty} \frac{d\omega}{\pi} \text{Im} \left[\int \frac{d\omega^3}{\pi^3} \frac{\rho_F(-\omega_1)}{\omega - \omega_1 + i\eta} \frac{\rho_F(-\omega_2) \rho_B(\omega_3)}{(\omega - \omega_2 - \omega_3 + i\eta)^2} (\text{sgn}(\omega_2) + \text{sgn}(\omega_3)) \right]. \end{aligned} \tag{B9}$$

Here the spectral functions are given by $\rho_F(\omega) = -\text{Im} G(\omega + i\eta)$ and $\rho_B(\omega) = \text{Im} D(\omega + i\eta)$. In our case we have for $0 < \omega \ll \omega_f$,

$$\begin{aligned} \rho_F(\pm\omega) &= -\text{Im} [G(\pm\omega + i\eta)] = \text{Im} [ie^{i\theta} \bar{\omega}_f^{x-1} (\mp i\omega)^{-x}] = \cos\left(\frac{\pi x}{2} \pm \theta\right) \bar{\omega}_f^{x-1} \omega^{-x}, \\ \rho_B(\pm\omega) &= \text{Im} [D(\pm\omega + i\eta)] = \text{Im} \left[\frac{1}{\bar{\beta} m_0^2} \left(\frac{\mp i\omega}{\bar{\omega}_f} \right)^{2x-1} \right] = \pm \frac{\cos(\pi x)}{\bar{\beta} m_0^2} \left(\frac{\omega}{\bar{\omega}_f} \right)^{2x-1}. \end{aligned} \tag{B10}$$

In the last step of Eq. (B9), we have used the fact $\rho_B(-\omega) = -\rho_B(\omega)$. On the other hand, $\rho_F(\omega)$ is asymmetric.

Averaging the second and the fifth lines of Eq. (B9), we get by separating the $\rho_F(\omega_1)\rho_F(\omega_2)$ into symmetric and antisymmetric parts

$$\begin{aligned} \frac{I_2}{\omega_0^3} &= \int_{-\infty}^{\infty} \frac{d\omega}{4\pi} \text{Im} \left[\int \frac{d\omega^3}{\pi^3} \frac{[\rho_F(\omega_1)\rho_F(\omega_2) + \rho_F(-\omega_1)\rho_F(-\omega_2)]\rho_B(\omega_3)}{(\omega - \omega_1 + i\eta)(\omega - \omega_2 - \omega_3 + i\eta)^2} (\text{sgn}(\omega_2) + \text{sgn}(\omega_3)) \right] \\ &+ \int_0^{\infty} \frac{d\omega}{2\pi} \text{Im} \left[\int \frac{d\omega^3}{\pi^3} \frac{[\rho_F(\omega_1)\rho_F(\omega_2) - \rho_F(-\omega_1)\rho_F(-\omega_2)]\rho_B(\omega_3)}{(\omega - \omega_1 + i\eta)(\omega - \omega_2 - \omega_3 + i\eta)^2} (\text{sgn}(\omega_2) + \text{sgn}(\omega_3)) \right]. \end{aligned} \quad (\text{B11})$$

The contour integral over x in the first line vanishes since all poles are on the same side. From Eq. (B10), the second line vanishes unless ω_1 and ω_2 have the same sign. We have

$$\begin{aligned} I_2 &= -\frac{\omega_F}{\bar{\beta}\bar{\omega}_f} \int_0^{\infty} \frac{d\omega}{\pi} \text{Im} \int_0^{\infty} \frac{d\omega^3}{4\pi^3} \frac{\sin(2\pi x) \sin(2\theta)}{\omega_1^x \omega_2^x \omega_3^{1-2x}} \\ &\times \frac{1}{(\omega - \omega_1 + i\eta)(\omega - \omega_2 - \omega_3 + i\eta)^2} \\ &= -\frac{x \sin(2\theta)}{\sin(\pi x)} \lim_{\eta \rightarrow 0} \int_0^{\infty} \frac{d\omega}{\pi} \text{Im} \frac{1}{\omega + i\eta} = -\frac{x \sin(2\theta)}{2 \sin(\pi x)}. \end{aligned} \quad (\text{B12})$$

One may wonder if the different form of self-energy at high frequencies will contribute to a correction to the result, but we note that the contribution to the above result comes from $\omega \sim \eta$, thus the UV contribution is small $\mathcal{O}(\eta/\omega_0) = 0$. Hence this result is *exact*.

We have used the following identities:

$$\bar{\beta}\bar{\omega}_f = \beta\omega_f(1 + \alpha^2) = -\frac{\omega_F}{2\pi} \frac{\Gamma^2(-x)}{2\Gamma(-2x)}. \quad (\text{B13})$$

$$\int_0^{\infty} \frac{d\omega^3}{\omega_1^x \omega_2^x \omega_3^{1-2x}} \frac{1}{(y - \omega_1)(y - \omega_2 - \omega_3)^2} = \frac{\pi^{5/2} 4^x \csc(\pi x) \csc(2\pi x) \Gamma(1-x)}{y \Gamma(\frac{1}{2} - x)} \quad (\text{B14})$$

$$- \frac{(8\pi \Gamma(-2x))(2^{2x-1} \Gamma(1-x))}{x \Gamma(-x)^2 (\sqrt{\pi} \Gamma(\frac{1}{2} - x))} = 2. \quad (\text{B15})$$

Combining, we get

$$\begin{aligned} \nu &= \frac{1}{2} + \frac{\theta}{\pi} + \frac{x \sin(2\theta)}{2 \sin(\pi x)} = \frac{1}{2} + \frac{\tan^{-1} \alpha}{\pi} \\ &+ \frac{x}{2 \sin(\pi x)} \frac{2\alpha}{1 + \alpha^2}. \end{aligned} \quad (\text{B16})$$

This is Eq. (10) of the main text.

Remarkably, this result is identical to the complex SYK_q model, but here our x is continuously tunable. It may not immediately clear why I_2 is the same as the SYK model, which has very different structures. It turns out ν can also be directly derived from I_1 alone, by doing the calculations and regularization in the time domain, in which case $I_2 = 0$, as shown in Ref. [37]. Since I_1 only depends on fermion Green's function, our result should be the same as SYK_q model with the same scaling dimension for the fermions. The fact that $I_{1,2}$ separately depends on regularization scheme but their sum does not is also reminiscent of features in chiral anomaly.

We note in passing that if we used the power-law form for the self-energy, Eq. (A1) and computed $\nu =$

$\int_{-\infty}^{\infty} \frac{dz}{2\pi i} G(z) e^{z0_+}$, we would obtain instead

$$\nu = \frac{1}{2} + \frac{1}{\pi} \frac{\tan^{-1} \alpha}{1-x}. \quad (\text{B17})$$

This relation is similar, but not identical to the exact one, although both yield $\nu = 1$ for $\alpha \rightarrow 1$ and $x \rightarrow 1/2$.

We also note that if we combine (B17) with Eq. (A16) and the exact relations (7) and (6), we find that very near $\nu = 1$, μ actually increases with ν : $\mu = (\omega_F/2)(1 - 3.2(M/N)\sqrt{1-\nu})$, hence $\partial\nu/\partial\mu > 0$. Taken at the face value, this would imply that the transition between the incompressible and the NFL phase is second order for any N/M , and then there is a first-order transition within in NFL phase. However, this is likely an artifact of the approximation as we didn't detect this behavior in numerical studies.

APPENDIX C: THE ENDPOINT OF THE NFL SOLUTION

In this section, we analyze how the NFL solution vanishes at $x = 1/2$, in particular at which chemical potential μ it does so. In general, unlike the filling ν , the chemical potential cannot be analytically expressed by universal quantities. However we find that it takes a universal value at the end of the NFL solution, namely, as filling $\nu \rightarrow 1$. While the NFL phase as a stable state disappears through a first-order phase transition, the saddle-point solution to the Schwinger-Dyson equation exists beyond the first-order phase transition. In the limit where the first-order transition becomes second-order, such an endpoint of the NFL solution becomes a true quantum-critical point.

As was shown in the main text, at the endpoint of the NFL solution, $x \rightarrow 1/2$, $\alpha \rightarrow 1$, and $\beta\omega_f \rightarrow 0$. We know that the bosonic self-energy $\bar{\Pi}(i\Omega)$ at $\Omega \gtrsim \omega_f$ crosses over from $\beta m_0^2 |\Omega/\omega_f|^{1-2x}$ to the bare mass m_0^2 , which is only possible at $x \rightarrow 1/2$ for

$$\beta = 1, \quad \omega_f \rightarrow 0. \quad (\text{C1})$$

Notice that $\beta = 1$ is also obtained in Sec. A1. In this limiting case calculating $\Sigma(0)$ from the imaginary-time Green's functions can be difficult since the bosonic Green's function involves a 0^0 limit. However the spectral functions, whose IR behavior are shown in Eq. (B10), are free from this ambiguity.

The chemical potential is given in terms of spectral functions by

$$\begin{aligned} \mu &= -\Sigma(0) = -\omega_0^3 \int \frac{d\Omega}{2\pi} \int \frac{d\omega d\omega'}{\pi^2} \frac{\rho_B(\omega)\rho_F(\omega')}{(i\Omega - \omega)(i\Omega - \omega')} \\ &= -\omega_0^3 \int \frac{d\omega d\omega'}{2\pi^2} \frac{\rho_B(\omega)\rho_F(\omega')}{\omega - \omega'} \\ &\times [\text{sgn}(\omega) - \text{sgn}(\omega')]. \end{aligned} \quad (\text{C2})$$

At $x \rightarrow 1/2$, from Eq. (B10), we have at low energies ($0 < \omega \ll \bar{\omega}_f$)

$$\begin{aligned}\rho_F(\pm\omega) &= \cos\left(\frac{\pi x}{2} \pm \theta(x)\right) \bar{\omega}_f^{-1/2} \omega^{-1/2}, \\ \rho_B(\pm\omega) &= \pm \frac{\cos(\pi x)}{\beta m_0^2} \left(\frac{\omega}{\bar{\omega}_f}\right)^{2x-1}.\end{aligned}\quad (\text{C3})$$

Notice that in the $x \rightarrow 1/2$ limit the low-energy bosonic spectral weight gets progressively depleted. This indeed matches the starting point of the gapped phase, in which bosons are gapped at the bare mass and the chemical potential gets renormalized to zero. In other words, upon entering the NFL phase, the boson mass gap “fills in” rather than “closes in.” We have showed the behavior of the spectral functions ρ_B in Fig. 3 of the main text.

Going back to the NFL side, since all the bosonic spectral weight is depleted at low frequencies, at $x \rightarrow 1/2$, ρ_B is peaked at high energies, and in this regime, the bosons behave like free ones. We have

$$\rho_B(\pm\omega) = \pm \pi \delta(\omega - m_0)/(2m_0). \quad (\text{C4})$$

Thus

$$\mu = -\frac{\omega_0^3}{2m_0} \left[\int_{-\infty}^0 \frac{d\omega'}{\pi} \frac{\rho_F(\omega')}{m_0 - \omega'} - \int_0^{\infty} \frac{d\omega'}{\pi} \frac{\rho_F(\omega')}{m_0 + \omega'} \right]. \quad (\text{C5})$$

In the weak-coupling limit, the width of $|\rho_F(\omega)|$ in frequency is the scale of interaction $\omega_f \ll m_0$. Thus approximately we

obtain

$$\begin{aligned}\mu &= -\frac{\omega_0^3}{2m_0^2} \int_0^{\infty} \frac{d\omega}{\pi} [\rho_F(-\omega) - \rho_F(\omega)] \\ &= \frac{\omega_0^3}{2m_0^2} (2\nu - 1) \Big|_{x=1/2}.\end{aligned}\quad (\text{C6})$$

In the last step, we have used $\nu = \int_0^{\infty} d\omega \rho_F(\omega)/\pi$ and $1 - \nu = \int_{-\infty}^0 d\omega \rho_F(\omega)/\pi$, which can be easily seen by a spectral decomposition of the fermionic Green's function.

We have now converted the calculation of μ to that of ν , to which one can apply the Luttinger theorem. From Eq. (B16) we have $\nu = 1$ at $x = 1/2$. Therefore we conclude as the NFL solution approaches its endpoint, the chemical potential tends to

$$\mu\left(x = \frac{1}{2}\right) = \frac{\omega_0^3}{2m_0^2} \equiv \frac{\omega_F}{2}, \quad (\text{C7})$$

which matches the starting point of the insulator phase. Interestingly, this result is also captured by using the power-law forms of the self-energies. Indeed, we see that the key ingredient for $\mu = \omega_F/2$ is the mismatch of fermionic and bosonic spectral weights at $x = 1/2$, which is also present even if one uses power-law forms of the self-energies. Of course, in the insulating phase the chemical potential can be obtained by the same procedures described here. However, this result does not hold for the strong-coupling case, where $\omega_0 \gg m_0$.

-
- [1] N. E. Hussey, A. P. Mackenzie, J. R. Cooper, Y. Maeno, S. Nishizaki, and T. Fujita, *Phys. Rev. B* **57**, 5505 (1998).
- [2] G. R. Stewart, *Rev. Mod. Phys.* **73**, 797 (2001).
- [3] T. Shibauchi, A. Carrington, and Y. Matsuda, *Annu. Rev. Condens. Matter Phys.* **5**, 113 (2014).
- [4] B. Keimer, S. A. Kivelson, M. R. Norman, S. Uchida, and J. Zaanen, *Nature (London)* **518**, 179 (2015).
- [5] C. M. Varma, P. B. Littlewood, S. Schmitt-Rink, E. Abrahams, and A. E. Ruckenstein, *Phys. Rev. Lett.* **63**, 1996 (1989).
- [6] J. A. Hertz, *Phys. Rev. B* **14**, 1165 (1976); A. J. Millis, *ibid.* **48**, 7183 (1993).
- [7] V. Oganesyan, S. A. Kivelson, and E. Fradkin, *Phys. Rev. B* **64**, 195109 (2001); W. Metzner, D. Rohe, and S. Andergassen, *Phys. Rev. Lett.* **91**, 066402 (2003); L. Dell'Anna and W. Metzner, *Phys. Rev. B* **73**, 045127 (2006); J. Rech, C. Pépin, and A. V. Chubukov, *ibid.* **74**, 195126 (2006); D. L. Maslov and A. V. Chubukov, *ibid.* **81**, 045110 (2010); M. J. Lawler and E. Fradkin, *ibid.* **75**, 033304 (2007); A. V. Chubukov and D. V. Khveshchenko, *Phys. Rev. Lett.* **97**, 226403 (2006).
- [8] A. Abanov, A. V. Chubukov, and A. M. Finkel'stein, *Europhys. Lett.* **54**, 488 (2001); A. Abanov, A. V. Chubukov, and J. Schmalian, *Adv. Phys.* **52**, 119 (2003).
- [9] I. Vekhter and A. V. Chubukov, *Phys. Rev. Lett.* **93**, 016405 (2004); Y. Wang, A. Abanov, B. L. Altshuler, E. A. Yuzbashyan, and A. V. Chubukov, *ibid.* **117**, 157001 (2016).
- [10] H. v. Löhneysen, A. Rosch, M. Vojta, and P. Wölfle, *Rev. Mod. Phys.* **79**, 1015 (2007).
- [11] T. Senthil, *Phys. Rev. B* **78**, 035103 (2008).
- [12] M. A. Metlitski and S. Sachdev, *Phys. Rev. B* **82**, 075127 (2010); **82**, 075128 (2010).
- [13] H.-C. Jiang, M. S. Block, R. V. Mishmash, J. R. Garrison, D. N. Sheng, O. I. Motrunich, and M. P. A. Fisher, *Nature (London)* **493**, 39 (2013).
- [14] S. Raghu, G. Torroba, and H. Wang, *Phys. Rev. B* **92**, 205104 (2015).
- [15] S.-S. Lee, *Phys. Rev. B* **80**, 165102 (2009); *Annu. Rev. Condens. Matter Phys.* **9**, 227 (2018).
- [16] S. Lederer, Y. Schattner, E. Berg, and S. A. Kivelson, *Phys. Rev. Lett.* **114**, 097001 (2015); Y. Schattner, S. Lederer, S. A. Kivelson, and E. Berg, *Phys. Rev. X* **6**, 031028 (2016); X. Y. Xu, K. Sun, Y. Schattner, E. Berg, and Z. Y. Meng, *ibid.* **7**, 031058 (2017); A. Klein, Y. Schattner, E. Berg, and A. V. Chubukov, *arXiv:2003.09431* [cond-mat.str-el].
- [17] X. Y. Xu, A. Klein, K. Sun, A. V. Chubukov, and Z. Y. Meng, *arXiv:2003.11573* [cond-mat.str-el].
- [18] P. A. Lee and N. Nagaosa, *Phys. Rev. B* **46**, 5621 (1992).
- [19] B. I. Halperin, P. A. Lee, and N. Read, *Phys. Rev. B* **47**, 7312 (1993).
- [20] B. L. Altshuler, L. B. Ioffe, and A. J. Millis, *Phys. Rev. B* **50**, 14048 (1994); C. Nayak and F. Wilczek, *Nucl. Phys. B* **417**, 359 (1994); J. Polchinski, *ibid.* **422**, 617 (1994).
- [21] Y. B. Kim, P. A. Lee, and X.-G. Wen, *Phys. Rev. B* **52**, 17275 (1995); Y. B. Kim, P. A. Lee, X.-G. Wen, and P. C. E. Stamp, *ibid.* **51**, 10779 (1995).
- [22] J. K. Jain and P. W. Anderson, *Proc. Natl. Acad. Sci. U.S.A.* **106**, 9131 (2009).

- [23] D. F. Mross, J. McGreevy, H. Liu, and T. Senthil, *Phys. Rev. B* **82**, 045121 (2010); M. A. Metlitski, D. F. Mross, S. Sachdev, and T. Senthil, *ibid.* **91**, 115111 (2015).
- [24] D. Dalidovich and S.-S. Lee, *Phys. Rev. B* **88**, 245106 (2013).
- [25] J. A. Damia, S. Kachru, S. Raghun, and G. Torroba, *Phys. Rev. Lett.* **123**, 096402 (2019).
- [26] Y. Gu, X.-L. Qi, and D. Stanford, *J. High Energy Phys.* **05** (2017) 125.
- [27] X.-Y. Song, C.-M. Jian, and L. Balents, *Phys. Rev. Lett.* **119**, 216601 (2017).
- [28] D. Chowdhury, Y. Werman, E. Berg, and T. Senthil, *Phys. Rev. X* **8**, 031024 (2018); D. Chowdhury and E. Berg, *Phys. Rev. Res.* **2**, 013301 (2020).
- [29] X.-C. Wu, C.-M. Jian, and C. Xu, *Phys. Rev. B* **100**, 075101 (2019).
- [30] O. Can and M. Franz, *Phys. Rev. B* **100**, 045124 (2019).
- [31] S. Sachdev and J. Ye, *Phys. Rev. Lett.* **70**, 3339 (1993).
- [32] A. Kitaev, Talks at KITP, University of California, Santa Barbara, Entanglement in Strongly-Correlated Quantum Matter (2015).
- [33] S. Sachdev, *Phys. Rev. X* **5**, 041025 (2015).
- [34] J. Maldacena and D. Stanford, *Phys. Rev. D* **94**, 106002 (2016).
- [35] A. Kitaev and S. J. Suh, *J. High Energy Phys.* **05** (2018) 183.
- [36] A. Altland, D. Bagrets, and A. Kamenev, *Phys. Rev. Lett.* **123**, 106601 (2019).
- [37] Y. Gu, A. Kitaev, S. Sachdev, and G. Tarnopolsky, *J. High Energy Phys.* **05** (2020) 157.
- [38] R. A. Davison, W. Fu, A. Georges, Y. Gu, K. Jensen, and S. Sachdev, *Phys. Rev. B* **95**, 155131 (2017).
- [39] Y. Wang, *Phys. Rev. Lett.* **124**, 017002 (2020).
- [40] I. Esterlis and J. Schmalian, *Phys. Rev. B* **100**, 115132 (2019).
- [41] D. Hauck, M. J. Klug, I. Esterlis, and J. Schmalian, *Annals Phys.* **417**, 168120 (2020).
- [42] Y. Cao, V. Fatemi, A. Demir, S. Fang, S. L. Tomarken, J. Y. Luo, J. D. Sanchez-Yamagishi, K. Watanabe, T. Taniguchi, E. Kaxiras *et al.*, *Nature (London)* **556**, 80 (2018).
- [43] Y. Cao, V. Fatemi, S. Fang, K. Watanabe, T. Taniguchi, E. Kaxiras, and P. Jarillo-Herrero, *Nature (London)* **556**, 43 (2018).
- [44] A. I. Coldea and M. D. Watson, *Annu. Rev. Condens. Matter Phys.* **9**, 125 (2018).
- [45] G. Pan, Y. Wang, and Z. Y. Meng, *arXiv:2001.06586* [cond-mat.str-el].
- [46] Z. Bi, C.-M. Jian, Y.-Z. You, K. A. Pawlak, and C. Xu, *Phys. Rev. B* **95**, 205105 (2017).
- [47] X. Wu, X. Chen, C.-M. Jian, Y.-Z. You, and C. Xu, *Phys. Rev. B* **98**, 165117 (2018).
- [48] A. A. Patel, M. J. Lawler, and E.-A. Kim, *Phys. Rev. Lett.* **121**, 187001 (2018).
- [49] J. Kim, I. R. Klebanov, G. Tarnopolsky, and W. Zhao, *Phys. Rev. X* **9**, 021043 (2019).
- [50] Y. Cheipesh, A. I. Pavlov, V. Scopelliti, J. Tworzydło, and N. V. Gnedilov, *Phys. Rev. B* **100**, 220506 (2019).
- [51] H. Wang, A. L. Chudnovskiy, A. Gorsky, and A. Kamenev, *Phys. Rev. Research* **2**, 033025 (2020).
- [52] J. Kim, X. Cao, and E. Altman, *Phys. Rev. B* **101**, 125112 (2020).
- [53] G. Kotliar, S. Y. Savrasov, K. Haule, V. S. Oudovenko, O. Parcollet, and C. A. Marianetti, *Rev. Mod. Phys.* **78**, 865 (2006).
- [54] A. Georges, O. Parcollet, and S. Sachdev, *Phys. Rev. B* **63**, 134406 (2001).
- [55] T. Azezanagi, F. Ferrari, and F. I. S. Massolo, *Phys. Rev. Lett.* **120**, 061602 (2018).
- [56] A. A. Patel and S. Sachdev, *Phys. Rev. Lett.* **123**, 066601 (2019).
- [57] In a full self-consistent calculation with frequency-dependent $\Sigma(i\omega)$, $\Pi(i\Omega)$ is nonzero, but parameterically small compared to m_0^2 .
- [58] In this respect, NFL behavior in the Y-SYK model differs from that for dispersing itinerant fermions coupled to Landau-overdamped massless collective bosons, as there fermionic and bosonic self-energies do not change between frequencies, where $\Sigma(i\omega) > i\omega$, and $\Sigma(i\omega) < i\omega$.
- [59] The code for the iterative solution of the Schwinger-Dyson equations can be accessed at <https://sites.google.com/site/yuxuanwang111/quantum-phase-transition-in-the-yukawa-syk-model?authuser=0>.
- [60] https://en.wikipedia.org/wiki/Maxwell_construction.
- [61] C. L. Baldwin and B. Swingle, *arXiv:1911.11865* [cond-mat.dis-nn].
- [62] E. Tulipman and E. Berg, *arXiv:2004.03617* [cond-mat.str-el].
- [63] A. Kruchkov, A. A. Patel, P. Kim, and S. Sachdev, *Phys. Rev. B* **101**, 205148 (2020).
- [64] H. Guo, Y. Gu, and S. Sachdev, *Annal. Phys.* **418**, 168202 (2020).
- [65] J. M. Luttinger and J. C. Ward, *Phys. Rev.* **118**, 1417 (1960).
- [66] B. L. Altshuler, A. V. Chubukov, A. Dashevskii, A. M. Finkel'stein, and D. K. Morr, *Europhys. Lett.* **41**, 401 (1998).